

Rheological Properties of Wormlike Micelles Formed in Aqueous Systems of 3-Alkoxy-2-hydroxypropyl Trimethyl Ammonium Bromides in the Presence of Sodium Octanoate

Ali Ping¹ · Peipei Geng¹ · Xilian Wei¹ · Jie Liu¹ · Junhong Zhang¹ ·
Dezhi Sun¹ · Xiaodong Guo¹ · Min Yang¹

Received: 14 January 2015 / Accepted: 30 July 2015 / Published online: 18 August 2015
© AOCs 2015

Abstract The rheological properties of aqueous systems composed of each of the four homologous cationic surfactants (3-alkoxy-2-hydroxypropyl trimethyl ammonium bromides, C_n HTAB, $n = 12, 14, 16$ and 18) in the presence of an anionic surfactant, sodium octanoate (SO), have been studied by using steady state and frequency sweep rheological measurements. The effects of surfactant concentration, hydrophobic chain length and temperature were investigated. In C_{14} HTAB solution, the viscosity shows shear thinning in the concentration range of $C_{C_{14}HTAB} > 320$ mmol/kg. Addition of SO promotes the micellar growth and results in the generation of wormlike micelles. Zero-shear viscosity (η_0) of the binary surfactant system exhibits a maximum point in the investigated concentration range, suggesting the interaction between C_{14} HTAB and SO molecules is strongest at the optimal ratio of C_{14} HTAB with SO. The decrease in viscosity was attributed to be the transition from entangled wormlike micelles to branching micelles after the maximum point, cryo-TEM images revealed the changes in the structure of the wormlike micelles.

Keywords 3-Alkoxy-2-hydroxypropyl trimethyl ammonium bromide · Sodium octanoate · Rheological property · Wormlike micelles

Electronic supplementary material The online version of this article (doi:10.1007/s11743-015-1724-4) contains supplementary material, which is available to authorized users.

✉ Xilian Wei
weixilian@lcu.edu.cn; weixilian123@126.com

¹ Shandong Provincial Key Laboratory of Chemical Energy Storage and Novel Cell Technology, Liaocheng University, Liaocheng 252059, Shandong, People's Republic of China

Introduction

It is known that the mixtures of oppositely charged surfactants can self-assemble into such microstructures as micelles, vesicles, lamellae, columnar and the cubic mesophases, depending on the different groups and the shape of the surfactant molecules. Among these microstructures, viscoelastic wormlike micelles formed in surfactants and its mixed systems have many potential applications, thus, there has been much interest in studying the properties of the wormlike micelles, in particular those stimuli-responsive surfactants systems in recent years [1–6].

The addition of one oppositely charged surfactant, even a small amount, to another surfactant solution is expected to enhance the formation of wormlike micelles because counterions reduce the micellar surface potential via charge neutralization and also increases the ionic strength by virtue of the released counterions [7, 8]. Thus, the rheological property of the binary solution of cationic and anionic surfactants is better than that of either parent surfactant. However, so far studies on the rheological behavior of the aqueous mixed system of counterionic surfactants are rather scarce [9–13], and this is in contradiction to the increasing development of mixed wormlike micellar solutions both in fundamental and in practical aspects. Therefore, we focus our attention in this work on the interactions of such a class of cationic surfactants, 3-alkoxy-2-hydroxypropyl trimethyl ammonium bromides (referred to as C_n HTAB, $n = 12, 14, 16$ and 18) and a counterionic surfactant. One of the readily available anionic surfactant, sodium octanoate (SO), is selected to form a mixed wormlike micelles solution with C_{14} HTAB. The influences of the hydrophobic effect, electrostatic interaction and hydrogen bonding on the viscoelastic behaviors of charged wormlike micelles have been investigated. The obtained

experimental data should be helpful not only for a solid understanding of cationic/anionic surfactant mixed systems, but also for further broadening of the potential applications of these mixed systems in the fields of household chemicals and functional materials.

Experimental

Materials

3-Alkoxy-2-hydroxypropyl trimethyl ammonium bromides (C_n HTAB, $n = 12, 14, 16$ and 18) were synthesized in our laboratory according to the methods reported in the literature [14]. The products were purified by recrystallization from acetone five times, and then dried under a vacuum for 2 days. The purity of these products was confirmed by the $^1\text{H-NMR}$ spectrum and elemental microanalysis. The detailed descriptions are available in the Electronic Supplementary Information 1, 2 (ESI 1, 2). Sodium octanoate (SO, Aldrich Chemical Reagent Co.) was a special grade reagent and was used as received. The molecular structures are shown in Scheme 1.

Methods

Rheological Measurements

Samples were prepared by mixing C_n HTAB, SO and water at a given molality and were homogenized by a magnetic stirrer at $50\text{ }^\circ\text{C}$, and then they were stored in a constant temperature water bath at $25\text{ }^\circ\text{C}$ to equilibrate. A stress controlled rheometer (AR2000ex, TA instruments, USA) with cone-plate geometry of 2° cone angle and 20 mm diameter was used for rheological measurements. The gap between the center of the cone and plate was $50\text{ }\mu\text{m}$. The measuring unit was equipped with a temperature unit (Peltier plate) providing rapid change of the temperature and giving accurate temperature control (uncertainty: $\pm 0.05\text{ }^\circ\text{C}$) over an extended time. Frequency sweep measurements were performed in the linear viscoelastic regime

of the samples, as determined previously by dynamic stress sweep measurements for all samples, and the frequency (ω) varying from 0.01 to 100 rad/s. For the steady-shear experiments, an equilibration time of 90 s was given at each data point. Each measurement was repeated three times to ensure good reproducibility (the deviation was less than 1 %).

Cryogenic Transmission Electron Microscopy (Cryo-TEM)

Aggregate structures were determined by cryo-TEM. Samples for cryo-TEM measurement were prepared in a controlled environment vitrification system (CEVS, Cryoplunge TM3, Gatan, USA) at $25\text{ }^\circ\text{C}$ at 95 % relative humidity. A drop of solution ($1\text{--}5\text{ }\mu\text{l}$) was placed on a TEM grid covered with a perforated carbon film and blotted with a filter paper to form a thin solution film on the grid. Samples were quenched rapidly in liquid ethane to form a vitrified sample and then transferred to liquid nitrogen until examination and were examined on a JEOL JEM 1400 TEM operating at 120 kV. The cryo transfer holder temperature was maintained below $-166\text{ }^\circ\text{C}$ during imaging. Images were recorded on a high-resolution cooled CCD camera.

$^1\text{H-NMR}$ Measurements

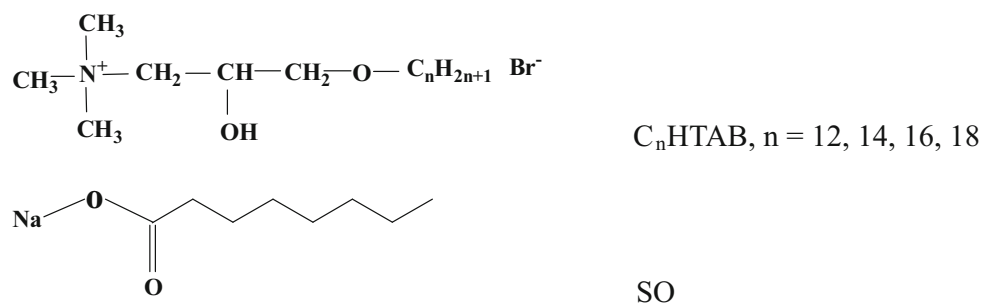
$^1\text{H-NMR}$ spectra of C_n HTAB were measured using an MP-400 nuclear magnetic resonance spectrometer (Varian Company, US) at the proton resonance frequency of 400.15 MHz. All spectra were determined in deuterium oxide containing TMS as an internal reference.

Results and Discussion

Effect of Surfactants Concentration

Transparent viscoelastic solutions were formed in all determined samples and a systematic study was carried out using steady state and frequency sweep rheological

Scheme 1 The molecular structures of C_n HTAB ($n = 12, 14, 16, 18$) and SO



measurements. The steady shear viscosities of pure C_{14} -HTAB aqueous solutions at different concentrations are shown in Fig. 1 at 25.0 ± 0.2 °C. At low concentrations, these solutions form spherical micelles with very low viscosity and show Newtonian fluid behavior. However, when the surfactant concentration were higher than 320 mmol/kg, the systems formed long micelles, which can be proved from shear thinning behavior in steady shear viscosity [15, 16]. When SO was added to C_{14} -HTAB aqueous solution at 100 mmol/kg, the area per head group of each monomers markedly decreased due to the ion pairing formation which facilitates long micelles formation. The long micelle solution had higher viscosity than that of the system in the absence of SO and the steady shear viscosity exhibited shear thinning behavior (steady shear viscosity of C_{14} -HTAB/SO is shown in ESI 3). By extrapolating the plateau value, the zero-shear viscosity (η_0) at different SO concentrations were obtained and are shown in Fig. 2. It was observed that with increasing concentration of SO, the η_0 increases quickly and reaches a maximum at 60 mmol/kg SO and then decreases at high SO concentration. The maximum η_0 value (214.3 Pa·s) is 5 orders of magnitude

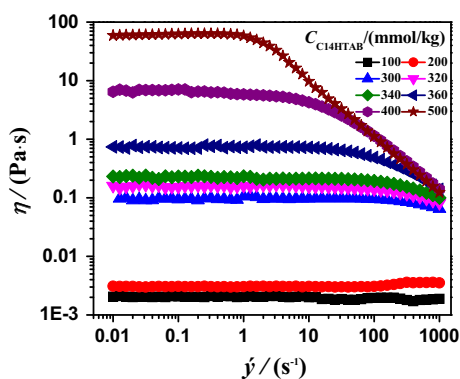


Fig. 1 Plot of steady shear viscosity (η) versus shear rate ($\dot{\gamma}$) as a function of C_{14} -HTAB concentration at 25 °C

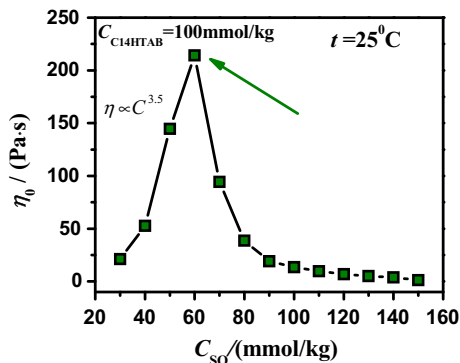


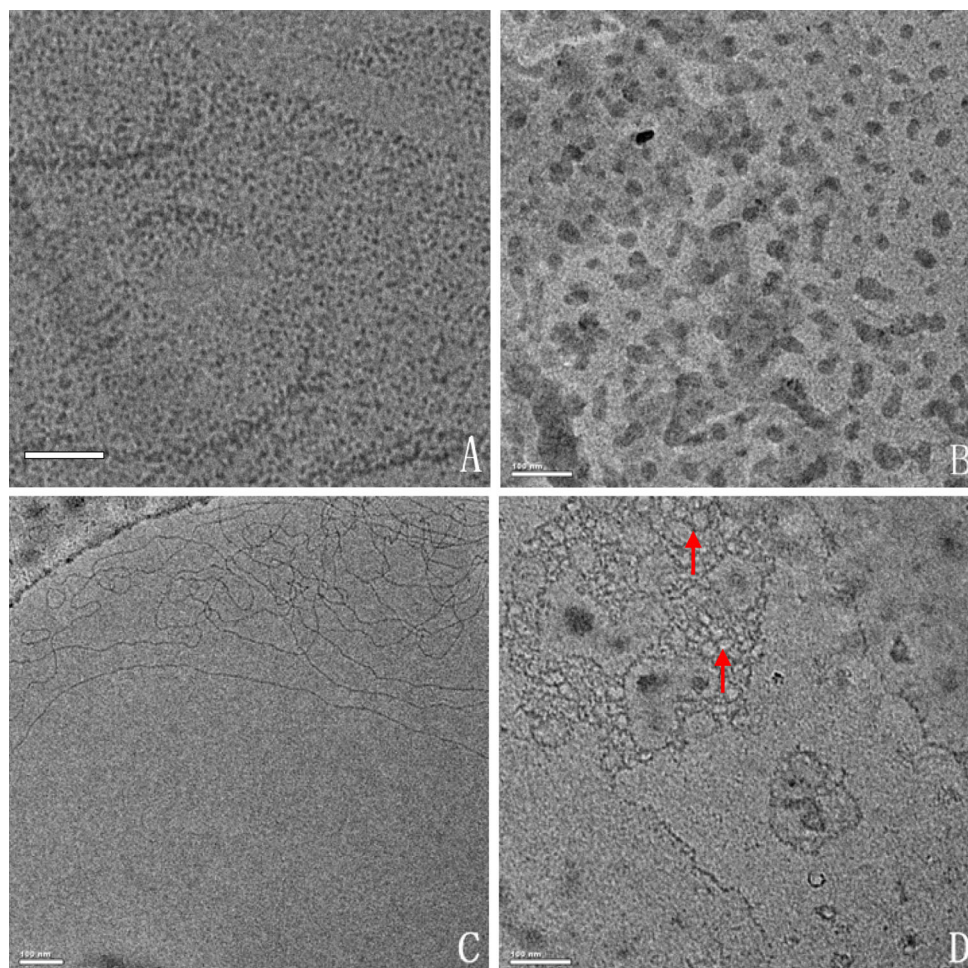
Fig. 2 Zero-shear viscosity of C_{14} -HTAB/SO aqueous solutions versus SO concentration at surfactant concentration of 100 mmol/kg ($t = 25$ °C)

larger than its initial viscosity without SO (0.002 Pa·s). The relationship between η_0 and SO concentration obeys the power law, $\eta_0 \propto C^{3.49}$ before the maximum, which was close to those wormlike micelles formed by nonionic surfactants investigated by Cates and co-workers (about 3.5) [17, 18]. The similar curve of a single pronounced peak was also observed in other cationic surfactant systems [7, 11–13, 19] and some conventional ionic surfactant/salt aqueous systems [20, 21]. For the viscosity going through a maximum as a function of surfactant ratio or salt content, there are two hypotheses in the literature. The first is that the micelles grow up to the peak and shrink beyond the peak [22–24]. The second hypothesis is that the micelles grow while staying linear up to the peak, remain linear micelles transform into a branched networks structure [8, 11, 15, 25–27] as observed from the presence of 3-way connections on the Cryo-TEM images [19, 27, 28]. Theoretical studies have predicted that branching of wormlike micelles should lower the viscosity [29]. For our system, the addition of the SO screens the interaction between the head groups and promotes an increase in micellar size, which further gives rise to an entangled network of wormlike micelles, but decreases η_0 surpassing the maximum. For the decision on which model described above is right, Raghavan pointed out that the most reliable way to confirm branches in wormlike micelles is the technique of cryo-transmission electron microscopy (cryo-TEM). In order to further confirm the structural changes in the micelle, we completed the cryo-TEM experiments. Photographs for several typical samples of the 100 mmol/kg C_{14} -HTAB solutions containing different relative amount of SO, 0, 40, 60 and 70 mmol/kg, respectively, are shown in Fig. 3.

Figure 3a shows that some spherical micelles exist in the system, their diameter is smaller than 10 nm. When SO is added to the system (Fig. 3b, 40 mmol/kg SO), the micrograph shows a number of cylindrical micelles of different length. In Fig. 3c, very long wormlike micelles are observed in the system, some wormlike micelles overlap and become entangled. As a consequence, it is impossible to identify where they begin and end. After the maximum (Fig. 3d), a micellar network formed by branched micelles was found and the micrograph shows a number of three-dimensional connections (red arrows). So the results from the cryo-TEM observation support the second hypothesis for our system in which the decrease in viscosity was attributed to be a shift from entangled wormlike micelles to branched micelles, which was in good agreement with the results from the steady shear rheology.

Significantly, the maximum viscosity occurs at a mole ratio of $C_{SO}/C_{C_{14}HTAB}$ about 0.6 where one SO molecule

Fig. 3 Cryo-TEM micrographs of wormlike micelles formed by C_{14} HTAB (100 mmol/kg) with **a** no SO, **b** 40 mmol/kg SO, **c** 60 mmol/kg SO, and **d** 70 mmol/kg SO. Scale bar 100 nm



roughly connects with two C_{14} HTAB molecules in the micelle (illustrated in Fig. 2). The peak shows the optimal composition of C_{14} HTAB and SO for the formation of the longest micelle or the strongest network structure. Obviously, it does not reflect an optimal extent of charge neutralization in the micelle where the counterions of C_{14} HTAB micelle are substituted completely by SO anions. A possible mechanism for the micellar branching may come from the transition of curvature of the micellar interface. The curvature of the aggregate is strongly influenced by the packing parameter p :

$$p = v/la \quad (1)$$

where v is the hydrophobic volume, l is the hydrophobic chain length of the surfactant molecule, and a the head group area of that molecule. When p is between $1/3$ and $1/2$, the surfactant molecules will be packed into cylindrical micelles. When p is between $1/2$ and 1 , flexible bilayers or vesicles form [30]. Wormlike micelles correspond to a locally cylindrical geometry with two end caps that are generally thought to be of hemispherical geometry having higher curvature. At low SO concentrations, the

electrostatic repulsion between headgroup of C_{14} HTAB molecules are partially screened and short rodlike micelles are formed which have a weak rheological response (low viscosity). As the SO content is increased, because of the strong interaction between C_{14} HTAB and SO, a is reduced and thus the packing parameter is increased, micelles grow rapidly into wormlike ones until the maximum. After that, continuing to increase SO to the solution, the electrostatic interactions are more effectively enhanced, the head group area could be further reduced and the tail volume increased. This provides favorable conditions for cross-link structure forming, rather than highly curved end-caps to promote branched micelle formation, leading to the decrease in zero shear viscosity. In addition, increasing the anionic surfactant concentration increases the concentration of counterions released into the solution. The effect is thus similar to salt addition and the maximum is initiated at a lower SO content for a higher C_{14} HTAB concentration. Such a mechanism could explain the observed results.

When $C_{SO} > 90$ mmol/kg, viscosity of the solution drops off slowly and then without obvious change,

suggesting that the long micelle is damaged gradually and the shape and structure of C₁₄HTAB/SO micelles change no further upon addition of SO. In an equimolar ratio, there are no precipitate or packed vesicles formation like those of cationic systems [8, 31, 32], indicating that a dense packing is sterically favorable for long micelles instead of precipitates or vesicles [10, 33, 34].

The frequency sweep is a popular method for studying the formation of long micelles or network structure. Figure 4 shows the dynamic rheological spectrum of 100 mmol/kg C₁₄HTAB/60 mmol/kg SO aqueous solution where the zero-shear viscosity shows a maximum (the dynamic rheological spectra of the 100 mmol/kg C₁₄HTAB and 30–150 mmol/kg SO are shown in ESI 4). Oscillatory shear measurements of viscoelastic micelles generally have single stress relaxation time (τ_R) at low shear frequency which is consistent with Maxwell fluids. The storage modulus (G'), and the loss modulus (G''), are given by the following relations [35–38].

$$G' = \frac{(\omega\tau_R)^2}{1 + (\omega\tau_R)^2} G'_\infty \quad (2)$$

$$G'' = \frac{\omega\tau_R}{1 + (\omega\tau_R)^2} G''_\infty \quad (3)$$

τ_R is obtained from ω_C^{-1} , and G' is equal to G'' in the frequency ω_C . At high ω , G' becomes a constant plateau module. Figure 3a represents a good fitting result for the typical case of 100 mmol/kg C₁₄HTAB/60 mmol/kg SO aqueous solution in the range of low and medium frequencies (solid lines). Viscous modulus (G'') appears as a maximum in ω_C , then decreases, and then passes through a minimum with increasing frequency. After this minimum, G'' increases again indicating at least a second relaxation time at a frequency beyond the limit of the rheometer (100 rad s⁻¹), but there is not enough high-frequency data to accurately determine the second maximum in the

process of our measurements. The semicircular curve of $G''-G'$ is another way of verifying viscoelastic wormlike micelles behavior [38]. It can be expressed as Eq. (4).

$$G''^2 + \left(G' - \frac{G_0}{2}\right)^2 = \left(\frac{G_0}{2}\right)^2 \quad (4)$$

Figure 4b shows the Cole–Cole plot from the data presented in Fig. 4a, and the solid lines correspond to Maxwellian evolution. Compared with the standard model, the experimental curve of $G''-G'$ behaves as a Maxwell fluid, having stress relaxation behavior characterized by a single terminal relaxation time except for G'' at high angular frequencies. We can see a departure in the measured evolution corresponding to the contribution of the breathing and Rouse modes. This accord with the fact that wormlike micelles are in a dynamic equilibrium and in the rapid breaking and recombination processes [35, 39, 40].

In this mixed system the directive driving force of long micelle-formation comes mainly from the strong interaction between the two surfactants with opposite charges, including the hydrophobic effect and electrostatic attraction. Besides, the role of hydrogen bonding appears to merit attention. In our recent publications, the amphiphilic molecule with substituted hydroxyl group was used in studies to analyze the effect of intermolecular hydrogen bonding on the wormlike formation. It was found that the intermolecular hydrogen bonding interaction increased the cohesive strength between the molecules and sped up the micellar growth [41]. In this work, C₁₄HTAB molecule and SO molecule contain respectively the hydroxypropyl group and carboxy group, so hydrogen-bonding interactions among the C₁₄HTAB, SO and water molecules possibly play an important role for the wormlike micelle formation.

When the concentration of SO is fixed at 60 mmol/kg (corresponding to the peak in Fig. 2), the solution of 60 mmol/kg SO is Newtonian fluid, the zero-shear viscosities and the plateau modulus of C₁₄HTAB/SO mixed solutions monotonically increase with increasing C₁₄HTAB concentration and show the power law dependence with the exponents of 1.3 and 0.96 (shown in Fig. 5), respectively. While the relaxation time τ_R as a function of C₁₄HTAB concentration exhibits a downtrend in a power law -2.59 (inserted figure). Although the rheological properties are monotonic functions of C₁₄HTAB concentration, the behavior still does not follow that predicted for ionic micelles. All exponents are very low compared with the theoretical value which predicted by Turner in some reversible scission wormlike micelles [36], namely, $\eta_0 \propto C^{3.7}$, $G_0 \propto C^{2.3}$ and $\tau_R \propto C^{1.3}$. This is a behavior of typical polyelectrolyte solutions that the increasing in η_0 and decreasing in τ_R with increasing surfactant concentration [21]. These results are similar to that from mixed

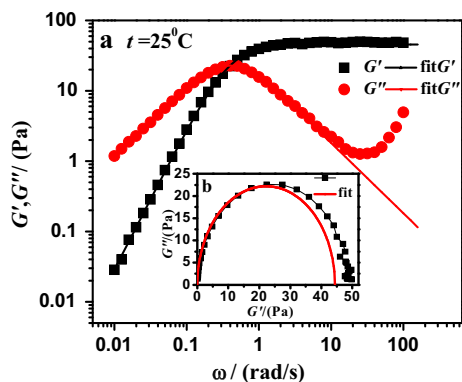


Fig. 4 Rheology of the system 100 mmol/kg C₁₄HTAB/60 mmol/kg SO: **a** dynamic frequency spectrum; **b** Cole–Cole plot at 25 °C (solid lines indicate the best fitting of the Maxwell model)

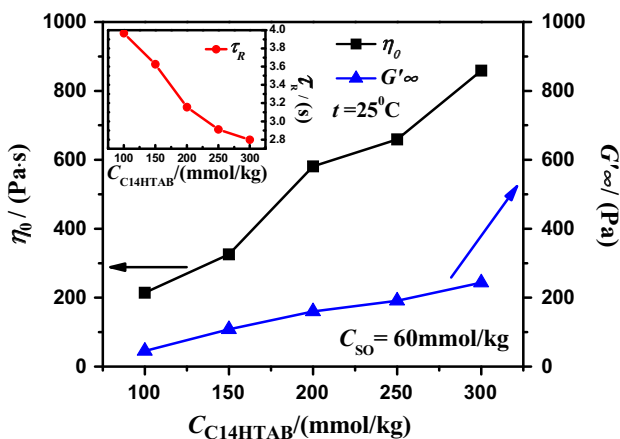


Fig. 5 Zero-shear viscosity η_0 , plateau modulus G'_∞ and relaxation time τ_R as a function of $C_{14}\text{HTAB}$ concentration at 25 °C, respectively

solution of CTAT/SDBS and a fixed sodium dodecylbenzenesulfonate concentration [39]. The increase of viscosity can be taken as evidence of micellar growth. The plateau modulus G'_∞ usually depends on the number density of the aggregates ρ_e by the equation $G'_0 = \rho_e K_B T$ [39]. The linearly increase of plateau modulus G'_∞ with the increasing $C_{14}\text{HTAB}$ corresponds to the increase of connection degree or branching and therefore reflects the decreasing mesh size ξ_M (shown in ESI 5) of the network. The increase of G'_∞ suggests that increasing $C_{14}\text{HTAB}$ concentration at the fixed $C_{14}\text{HTAB}/\text{SO}$ ratio does not radically alter the wormlike micellar structure in the examined concentration range, only decreasing the crimp degree of wormlike micelles.

Kaler had mentioned that the total persistence length of ionic micelles, l_p can be calculated from the intrinsic persistence length, l_p^0 , and electrostatic contribution, l_p^e , by the formula $l_p = l_p^0 + l_p^e$ [8]. The electrostatic persistence length, l_p^e , depended on micellar charge and Debye length, k^{-1} . The mean distance between charged groups L_0 and k^{-1} determine l_p^e according to the Odijk–Skolnick–Fixman (OSF) theory, as $l_p^e = (l_B/4)(k^{-1}/L_0)^2$, here l_B is the Bjerrum length. Thus in this mixed system increasing $C_{14}\text{HTAB}$ concentration decreases the k^{-1} , results in a decrease of l_p and reduces the longest relaxation time, τ_R .

Effect of the Alkyl Chain Length of the Surfactant

As a comparison, we investigated the behaviors of cationic surfactants with different alkyl chain length. The aqueous solutions of 100 mmol/kg $C_n\text{HTAB}$, $n = 12, 14, 16$ and 18, coexisting with 60 mmol/kg SO were selected as model

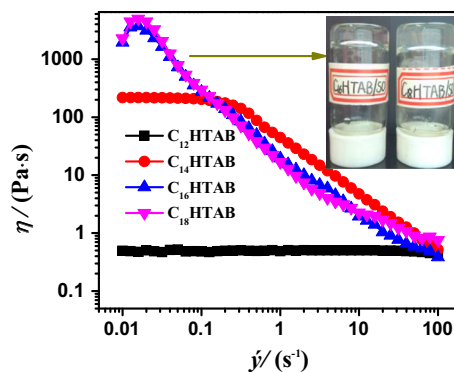


Fig. 6 Curves of apparent viscosity (η) versus shear rate ($\dot{\gamma}$) of 100 mmol/kg $C_n\text{HTAB}$ and 60 mmol/kg SO mixed aqueous solutions at 25 °C

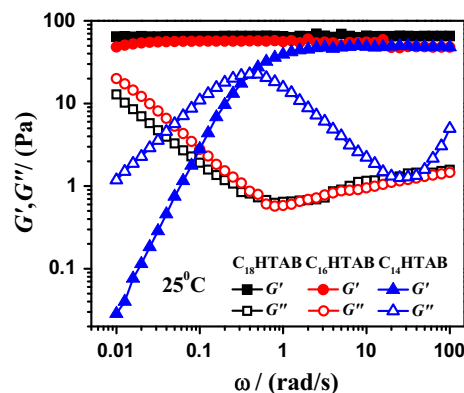


Fig. 7 Dynamic shear modulus G' and G'' obtained from frequency sweep measurements of 100 mmol/kg $C_{14-18}\text{HTAB}/60$ mmol/kg SO, $t = 25$ °C

systems. Figure 6 shows the steady shear viscosities of $C_{12-18}\text{HTAB}/\text{SO}$ aqueous solutions at 25 °C. The steady shear viscosity increase successively, on the whole, with increasing alkyl chain length. The steady shear viscosity of $C_{12}\text{HTAB}/\text{SO}$, however, shows Newtonian fluid behavior with low viscosity and that of $C_{14}\text{HTAB}/\text{SO}$ shows shear-thinning. For $C_{16-18}\text{HTAB}/\text{SO}$ solutions, we note that the curves of the shear viscosity vs shear rate display a sharp shear thickening at a very low shear rate (Fig. 5). The cause may be that the temperatures of both the solutions are lower than the Kraft point of the two surfactants (26 °C for $C_{16}\text{HTAB}$ and 32 °C for $C_{18}\text{HTAB}$). Although both the mixed systems seem to be transparent, the molecular chains of $C_{16}\text{HTAB}$ and $C_{18}\text{HTAB}$ are not fully extended, upon shear rate increasing, the interaction between $C_{16-18}\text{HTAB}$ and SO can be enhanced, and so peaks appear in the curves of shear viscosity vs shear rate (Fig. 6).

The dynamic shear modulus G' and G'' of 100 mmol/kg $C_{14-18}\text{HTAB}/60$ mmol/kg SO as a function of angular frequency at 25 °C are shown in Fig. 7. It can be seen that

no cross-over points can be detected for the samples $n = 16$ and 18, but the curves of G' have plateau and G' wholly exceed G'' throughout the examined frequencies, which is in accordance with the gel-like behavior [42, 43]. For the samples of $n = 14$, the changing trend of storage modulus (G') and loss modulus (G'') fits the Maxwell model and has the characteristic of wormlike micelles, *i.e.*, elastic modulus G' dominating over viscous modulus G'' at high ω and viscous modulus G'' dominating over elastic modulus G' at low ω [40]. While C_{12} HTAB/SO aqueous solution has not showed well elasticity. In other words, the C_n HTAB/SO mixed aqueous solutions change from Newtonian fluids to non-Newtonian fluids (solution of wormlike micelles), then to solutions of gel-like micelles with the increasing chain length of cationic hydrophobic group at 25 °C. These experimental results fully show that the hydrophobic interaction is strengthened with increasing alkyl chain length and long wormlike micelles and a gel is easier to form in the system. This gelation behavior may be attributed to the crystallization of wormlike micelles, which is related to the strong synergic interaction between both the surfactants under the Kraft point of C_{16-18} HTAB [44, 45]. When the temperature is increased to above 35 °C, both the samples exhibits characteristic wormlike micelle features with strong viscoelastic behavior.

Effect of Temperature

The viscoelasticity of 100 mmol/kg C_n HTAB/60 mmol/kg SO solution was studied from 15 to 35 °C. In the examined temperature range, a sample of 100 mmol/kg C_{12} HTAB/60 mmol/kg SO did not show good rheological behavior. Figure 7 shows the variation of the dynamic rheological properties of 100 mmol/kg C_{14-16} HTAB/60 mmol/kg SO as a function of angular frequency at different temperatures. For the sample 100 mmol/kg C_{14} HTAB/60 mmol/kg SO (Fig. 8a), G' dominates over G'' at high ω and G'' exceed G' at low ω , which is a typical viscoelastic response of wormlike micelles. And the ω value of the crossover point increases from 0.1834 rad s⁻¹ at 15 °C to 3.960 rad s⁻¹ at 35 °C, indicating a relaxation time decrease and viscoelasticity is damaged when the temperature of the sample is enhanced. The higher angular frequency at which G' and G'' cross, the faster the relaxation process of micelles and the more difficult is the formation of a network structure [36, 46] However the sample 100 mmol/kg C_{16} HTAB/60 mmol/kg SO (Fig. 8b) shows gel-like behavior at 15–25 °C and wormlike micelles behavior at 35 °C, indicating that the solution changes from gel-like to wormlike micelles with the increasing temperature. The dynamic rheological properties of 100 mmol/kg C_{18} HTAB/60 mmol/kg SO (shown in ESI 6) shows the same trend with that of C_{16} HTAB/SO system. These

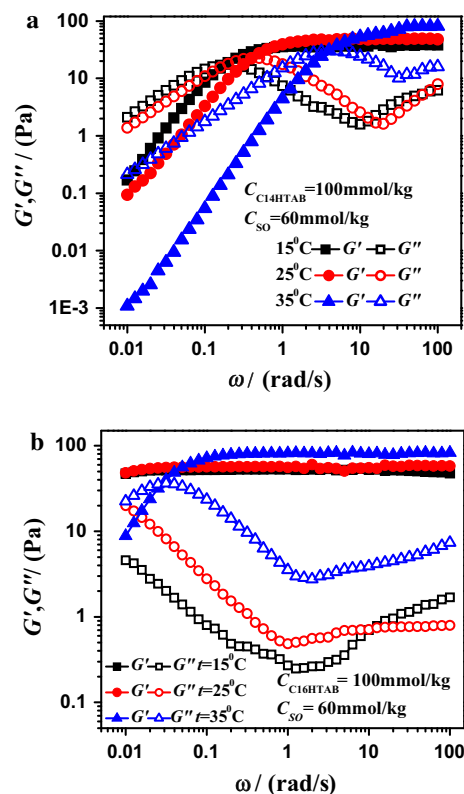


Fig. 8 Variations of G' and G'' with the shear frequency for 100 mmol/kg C_{14} HTAB (a), C_{16} HTAB (b) and 60 mmol/kg SO mixed aqueous solutions at different temperatures

experimental results of the above fully consistent with the expected results that thermodynamic free energy in turn reduce in the following order, C_{18} HTAB > C_{16} HTAB > C_{14} HTAB > C_{12} HTAB, *i.e.*, longer and more tightly packed micelles can be more easily formed at low temperature.

In addition, the steady shear viscosity is also investigated. For example, the viscosities of C_{14} HTAB/SO aqueous solutions at different temperatures show the typical shear thinning non-Newtonian fluid behavior. The zero-shear viscosities η_0 (shown in ESI 7) decrease successively with the increasing temperature, but the maximum η_0 value at $C_{SO} = 60$ mmol/kg does not change with a different temperature, indicating that the similar structure of micelles is in existence in our examined temperature range. It is easy to understand that the increasing thermal motion reduces the viscosity of the solution and decreases the average micellar length [22, 47]. The activation energy, E_a , can be obtained from the Arrhenius plot according to Eq. (5).

$$\eta_0 = Ae^{E_a/RT} \quad (5)$$

Activation energy, E_a is the necessary energy of an individual micelle to move in an environment of

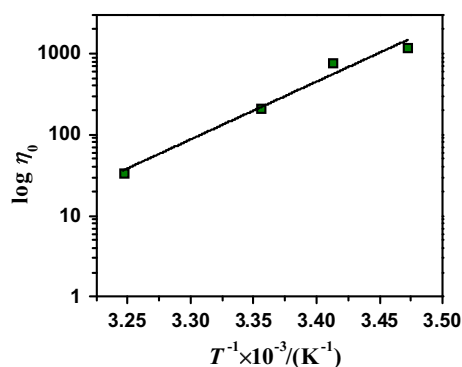


Fig. 9 Plot of η_0 (log scale) versus the reciprocal of the thermodynamic temperature for 100 mmol/kg C_{14} HTAB/60 mmol/kg SO mixed aqueous solutions

surrounding micelles. Therefore E_a is given by the interactions between individual aggregates [16]. Figure 9 presents the plot of $\ln \eta_0$ versus the reciprocal of the thermodynamic temperature for 100 mmol/kg C_{14} HTAB/60 mmol/kg SO mixed aqueous solutions. The plot is linear and demonstrates that the main η_0 follows Arrhenius-type behavior. A value of 136.35 kJ/mol for E_a obtained from the slope falls into the wide range of E_a values (70–300 kJ/mol) reported for surfactant micellar systems [27, 48–50].

Conclusion

In summary, the viscoelastic properties of C_n HTAB aqueous systems and their mixed solutions with SO were studied using viscosity measurements. Influences of surfactant concentration, alkyl chain length of C_n HTAB and temperature on the properties were investigated. In C_{14} -HTAB solution at 100 mmol/kg, only spherical micelles can be formed. The addition of SO can promote the micellar growth from spherical ones into rodlike ones and to wormlike ones by the synergistic effect of hydrophobic effect, electrostatic interaction and hydrogen bonds between the oppositely charged surfactants. Zero-shear viscosity of mixed solutions as a function of SO concentration shows a maximum peak behavior. The decrease in viscosity can be attributed to be the transition from entangled wormlike micelles to branching wormlike micelles after the maximum. Cryo-TEM observation confirmed the micellar structure changes with SO concentration increases. The viscosity and elasticity can be flexibly adjusted by selecting the suitable concentration, the ratio of the two surfactants, hydrophobic chain length of the surfactant molecule and the temperature. The steady and dynamic rheological curves show great differences with increasing the hydrophobic chain at a same ratio of

C_n HTAB/SO mixed solution. The activation energy, E_a , obtained from the Arrhenius plot falls into the range reported for surfactant micellar systems. These results may be regarded as an important reference in theoretical research and the practical application of mixed surfactants in several new fields.

Acknowledgments This work was supported by the National Natural Science Foundation of China and Shandong Province (Grant Nos. 21473084, 21073081, 21373106, ZR2012BQ013), Scientific Research, Experimental Technology (LDSY2014008) and Teaching Research Project of Liaocheng University (G20122036).

References

- Rogers SA, Calabrese MA, Wagner NJ (2014) Rheology of branched wormlike micelles. *Curr Opin Colloid Interface* 19:530–535
- Han YX, Feng YJ, Sun HQ, Li ZQ, Han YG, Wang HY (2011) Wormlike micelles formed by sodium erucate in the presence of a tetraalkylammonium hydrotrope. *J Phys Chem B* 115:6893–6902
- Tian MZ, Zhu LY, Yu DF, Wang YY, Sun SF, Wang YL (2013) Aggregate transitions in mixtures of anionic sulfonate gemini surfactant with cationic ammonium single-chain surfactant. *J Phys Chem B* 117:433–440
- Mitrinova Z, Tcholakova S, Popova Z, Denkov N, Dasgupta BR, Ananthapadmanabhan KP (2013) Efficient control of the rheological and surface properties of surfactant solutions containing C_8 - C_{18} fatty acids as cosurfactants. *Langmuir* 29:8255–8265
- Chu ZL, Dreiss CA, Feng YJ (2013) Smart wormlike micelles. *Chem Soc Rev* 42:7174–7203
- Yan H, Long Y, Song K, Tung CH, Zheng LQ (2014) Photo-induced transformation from wormlike to spherical micelles based on pyrrolidinium ionic liquids. *Soft Matter* 10:115–121
- Koehler RD (2000) Microstructure and Dynamics of wormlike micellar solutions formed by mixing cationic and anionic surfactants. *J Phys Chem B* 104:11035–11044
- Kaler EW, Herrington KL, Murthy AK, Zasadzinski JAN (1992) Phase behavior and structures of mixtures of anionic and cationic surfactants. *J Phys Chem* 96:6698–6707
- Blanco E, Rodríguez-Abreu C, Schulz P, Ruso JM (2010) Effect of alkyl chain asymmetry on catanionic mixtures of hydrogenated and fluorinated surfactants. *J Colloid Interface Sci* 341:261–266
- Li HG, Hao JC (2008) Phase behavior and rheological properties of a salt-free catanionic surfactant TTAOH/LA/ H_2O system. *J Phys Chem B* 112:10497–10508
- Raghavan SR, Fritz G, Kaler EW (2002) Wormlike micelles formed by synergistic self-assembly in mixtures of anionic and cationic surfactants. *Langmuir* 18:3797–3803
- Yin HQ, Lin YY, Huang JB (2009) Microstructures and rheological dynamics of viscoelastic solutions in a catanionic surfactant system. *J Colloid Interface Sci* 338:177–183
- Fan HM, Yan Y, Li ZC, Xu Y, Jiang LX, Xu LM, Zhang B, Huang JB (2010) General rules for the scaling behavior of linear wormlike micelles formed in catanionic surfactant systems. *J Colloid Interface Sci* 348:491–497
- Wei ZB, Wei XL, Wang XH, Wang ZN, Liu J (2011) Ionic liquid crystals of quaternary ammonium salts with a 2-hydroxypropoxy insertion group. *J Mater Chem* 21:6875–6882
- Acharya DP, Kunieda H (2003) Formation of viscoelastic wormlike micellar solutions in mixed nonionic surfactant systems. *J Phys Chem B* 107:10168–10175

16. Shrestha RG, Shrestha LK, Aramaki K (2007) Formation of wormlike micelle in a mixed amino-acid based anionic surfactant and cationic surfactant systems. *J Colloid Interface Sci* 311:276–284
 17. Cates ME, Marques CM, Bouchaud JP (1991) Dynamic relaxation of rodlike micelles. *J Chem Phys* 94:8529–8536
 18. Kern F, Lemarecha P, Candau SJ, Cates ME (1992) Rheological properties of semidilute and concentrated aqueous solutions of cetyltrimethylammonium bromide in the presence of potassium bromide. *Langmuir* 8:437–440
 19. Ziserman L, Abezgauz L, Ramon O, Raghavan SR, Danino D (2009) Origins of the viscosity peak in wormlike micellar solutions. 1. mixed cationic surfactants. A cryo-transmission electron Microscopy Study. *Langmuir* 25:10483–10489
 20. Cappelaere E, Cressely R (1998) Rheological behavior of an elongated micellar solution at low and high salt concentrations. *Colloid Polym Sci* 276:1050–1056
 21. Pei XM, Zhao JX, Ye YZ, You Y, Wei XL (2011) Wormlike micelles and gels reinforced by hydrogen bonding in aqueous cationic gemini surfactant systems. *Soft Matter* 7:2953–2960
 22. Magid LJ (1998) The surfactant-polyelectrolyte analogy. *J Phys Chem B* 102:4064–4074
 23. Cappelaere E, Cressely R (2000) Influence of NaClO₃ on the rheological behaviour of a micellar solution of CPCl. *Rheol Acta* 39:346–353
 24. Imae T, Kohsaka TJ (1992) Size and electrophoretic mobility of C₁₄TASal micelles in aqueous media. *Phys Chem* 96:10030–10035
 25. Croce V, Cosgrove T, Dreiss CA, King S, Maitland G, Hughes T (2005) Giant micellar worms under shear: a rheological study using SANS. *Langmuir* 21:6762–6768
 26. Candau SJ, Khatory A, Lequeux F, Kern F (1993) Rheological behaviour of wormlike micelles: effect of salt content. *J Phys IV* 3:197–209
 27. Croce V, Cosgrove T, Maitland G, Hughes T, Karlsson GR (2003) Rheology, Cryogenic transmission electron spectroscopy, and small-angle neutron scattering of highly viscoelastic wormlike micellar solutions. *Langmuir* 19:8536–8541
 28. Lin Z (1996) Branched worm-like micelles and their networks. *Langmuir* 12:1729–1737
 29. Lequeux F (1992) Reptation of connected wormlike micelles. *Europhys Lett* 19:675–681
 30. Israelachvili JN, Mitchell DJ, Ninham BW (1976) Theory of self-assembly of hydrocarbon amphiphiles into micelles and bilayers. *J Chem Soc Faraday Trans II* 72:1525–1568
 31. Puvvada S, Blankschtein D (1992) Mixed surfactant systems and Modeling mixed surfactant systems. In: Holland PM, Rubingh DN (eds) *Mixed surfactant systems*. ACS symposium series 501, Chapters 1 and 2. American Chemical Society, Washington, DC
 32. Herrington KL, Kaler EW, Miller DD, Zasadzinski JA, Chiruvolu S (1993) Phase behavior of aqueous mixtures of dodecyltrimethylammonium bromide and sodium dodecyl sulfate. *J Phys Chem* 97:13792–13802
 33. Regev O, Khan A (1996) Alkyl chain symmetry effects in mixed cationic-anionic surfactant systems. *J Colloid Interface Sci* 182:95–109
 34. Schulz PC, Rodríguez JL, Minardi RM, Sierra MB, Morini MA (2006) Are the mixtures of homologous surfactants ideal? *J Colloid Interface Sci* 303:264–271
 35. Kern F, Lequeux F, Zana R, Candau SJ (1994) Dynamic properties of salt-free viscoelastic micellar solutions. *Langmuir* 10:1714–1723
 36. Turner MS, Marques C, Cates ME (1993) Dynamics of wormlike micelles: the bond-interchange reaction scheme. *Langmuir* 9:695–701
 37. Clausen TM, Vinson PK, Minter JR, Davis HT, Talmon Y, Miller WG (1992) Viscoelastic micellar solutions: microscopy and rheology. *J Phys Chem* 96:474–484
 38. Gennee PGD (1979) *Scaling concepts in polymer physics*. Cornell University Press, Ithaca
 39. Ali AA, Makhoulfi R (1999) Effect of organic salts on micellar growth and structure studied by rheology. *Colloid Polym Sci* 277:270–275
 40. Schubert BA, Kaler EW, Wagner NJ (2003) The microstructure and rheology of mixed cationic/anionic wormlike micelles. *Langmuir* 19:4079–4089
 41. Khatory A, Lequeux F, Kern F, Candau SJ (1993) Linear and nonlinear viscoelasticity of semidilute solutions of wormlike micelles at high salt content. *Langmuir* 9:1456–1464
 42. Boris DC, Colby RH (1998) Rheology of sulfonated polystyrene solutions. *Macromolecules* 31:5746–5755
 43. Thurn H, Loebl M, Hoffmann H (1985) Viscoelastic detergent solutions—a quantitative comparison between theory and experiment. *J Phys Chem* 89:517–522
 44. Lin YY, Qiao Y, Tang PF, Li ZB, Huang JB (2011) Controllable self-assembled laminated nanoribbons from dipeptide-amphiphile bearing azobenzene moiety. *Soft Matter* 7:2762–2769
 45. Mu JH, Li GZ, Wang ZW (2002) Effect of surfactant concentration on the formation and viscoelasticity of anionic wormlike micelle by the methods of rheology and freeze-fracture TEM. *Rheol Acta* 41:493–499
 46. Cates ME, Candau SJ (1990) Statics and dynamics of worm-like surfactant micelles. *J Phys: Condens Matter* 2:6869–6892
 47. Kern F, Zana R, Candau J (1991) Rheological properties of semidilute and concentrated aqueous solutions of cetyltrimethylammonium chloride in the presence of sodium salicylate and sodium chloride. *Langmuir* 7:1344–1351
 48. Tung SH, Huang YE, Raghavan SR (2007) Contrasting effects of temperature on the rheology of normal and reverse wormlike micelles. *Langmuir* 23:372–376
 49. Yuan ZW, Lu WJ, Hao JC (2008) Gel phase originating from molecular quasi-crystallization and nanofiber growth of sodium laurate–water system. *Soft Matter* 4:1639–1644
 50. Lin YY, Qiao Y, Yan Y, Huang JB (2009) Thermo-responsive viscoelastic wormlike micelle to elastic hydrogel transition in dual-component systems. *Soft Matter* 5:3047–3053
- Ali Ping** is a master's student at Liaocheng University in China, and is studying at the School of Chemistry and Chemical Engineering. Her research deals with the synthesis of surfactants and properties of stimuli-responsive viscoelastic fluids.
- Peipei Geng** is a master's student at Liaocheng University in China, and is studying at the School of Chemistry and Chemical Engineering. Her research deals with the properties of stimuli-responsive viscoelastic fluids.
- Xilian Wei** is a professor at Liaocheng University in China. Her research interests include the synthesis of surfactants, building of the smart micelle, application and development of functional surfactants.
- Jie Liu** received her Ph.D. from the Key Laboratory of Colloid and Interface Chemistry, Shandong University, Ministry of Education, China. She is an associate professor at Liaocheng University in China and her research field is the properties of surfactants and ionic liquids.
- Junhong Zhang** received her Ph.D. from the Ocean University of China. She is an associate professor at Liaocheng University in China and her research field is the synthesis technology of surfactants.

Dezhi Sun is a professor at Liaocheng University in China. He received his Ph.D. degree in physical chemistry at Zhejiang University. His research field is chemical thermodynamics of colloids and interfaces.

Min Yang is an undergraduate at Liaocheng University in China. Her research deals with the properties of stimuli-responsive viscoelastic fluids.

Xiaodong Guo is an undergraduate at Liaocheng University in China. His research deals with the synthesis of surfactants.